A Robust, High-Content NAM for Repeatable and Predictive Developmental and Reproductive Toxicity Assessment in *C. elegans*

Sudip Mondal[1], Adam Laing[1], Amber Shen[1], Evan Hegarty[1], Abhishri Medewar[1], Sebastian Gomez[1], Gina Carrion[1], Julia Brown[1], and Adela Ben-Yakar[2,3]

[1]vivoVerse, LLC, Austin, TX 78731, USA
[2]Department of Mechanical Engineering, The University of Texas at Austin, TX 78712, USA
[3]Department of Biomedical Engineering, The University of Texas at Austin, TX 78712, USA

Supplementary information

Supplementary Figure 1: Overview of vivoScreen technology platform and imaging workflow using vivoChip.

Supplementary Figure 2. Screenshot of the vivoImager software during automated imaging of a vivoChip-24x device

Supplementary Figure 3: vivoChip-24x automated imaging workflow.

Supplementary Figure 4: Screenshot of the vivoAnalyzer software for embryo phenotyping.

Supplementary Figure 5: Workflow of statistical analysis for body and embryo phenotypes.

Supplementary Figure 6: An automated image acquisition and analysis pipeline to rapidly screen *C. elegans* models for DART studies**.**

Supplementary Figure 7. Dataset for U-Net-based body segmentation model.

Supplementary Figure 8: Dice score for the predicted worm segmentation.

Supplementary Figure 9: Example of *C. elegans* body segmentation.

Supplementary Figure 10. Well averages for all 6 DART parameters from one of the biological replicates.

Supplementary Figure 11. Variation in DART parameters across worms treated with four solvent conditions and five biological replicates.

Supplementary Figure 12: Range-finding assay with methylmercury.

Supplementary Figure 13: Representative images of methylmercury-treated worms.

Supplementary Figure 14: Concentration-response curve for methylmercury with 10 concentrations.

Supplementary Figure 15: Range-finding assay with propiconazole.

Supplementary Figure 16: Representative images of propiconazole-treated worms.

Supplementary Table 1: Predefined assay acceptance criteria for DART experiments.

Supplementary Table 2: Effective concentration values for DART-related parameters for methylmercury-treated worms.

Supplementary Table 3: Effective concentration values for DART-related parameters for methylmercury-treated worms with 10 concentrations.

Supplementary Table 4. Strictly Standardized Mean Difference values for different concentrations of methylmercury.

Supplementary Table 5. Effective concentration values for DART-related parameters for propiconazole-treated worms.

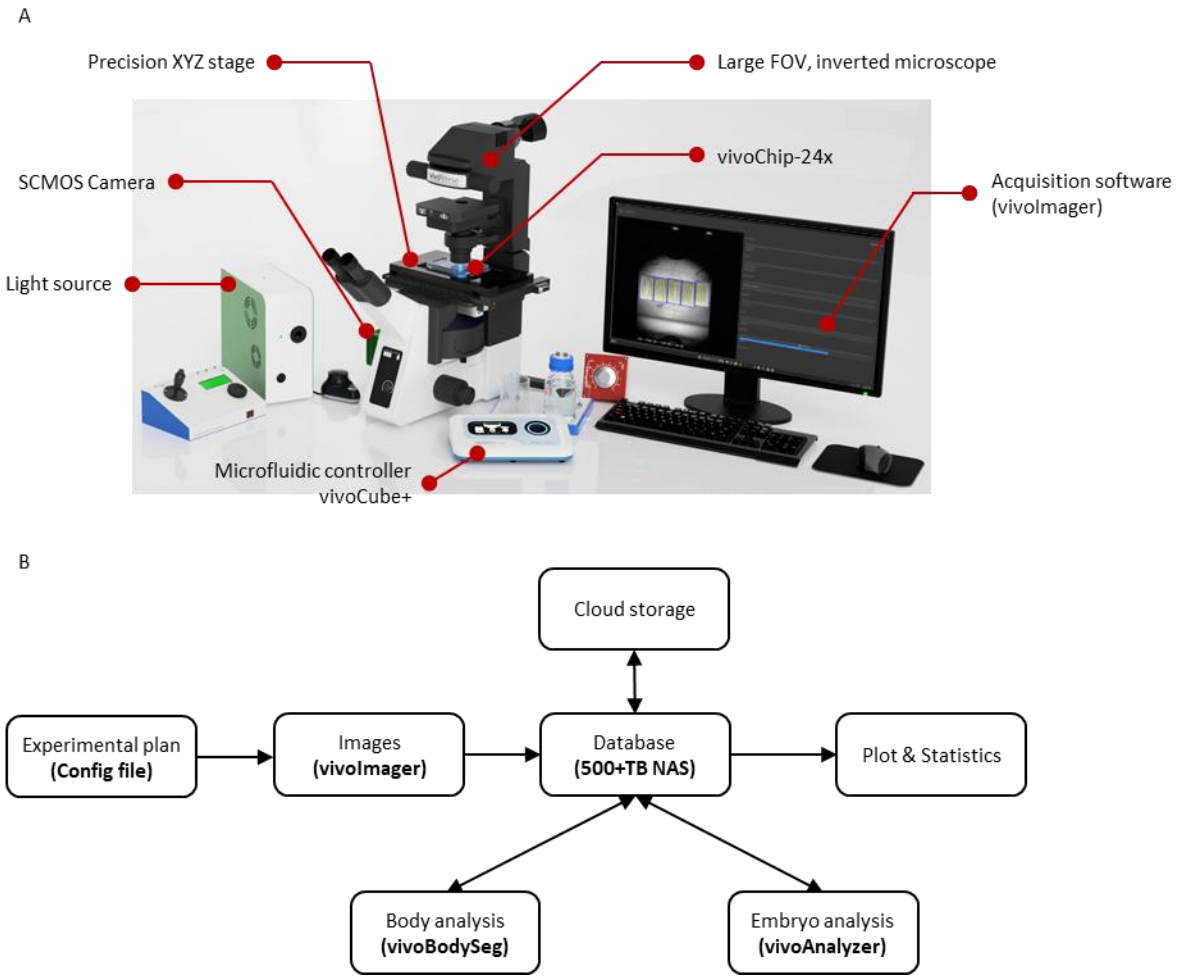

Supplementary Figure 1: Overview of vivoScreen technology platform and imaging workflow using vivoChip. (A) Schematic illustrating the main hardware components of the vivoScreen platform. The system comprises a customized inverted microscope, configured for large field-of-view (FOV) image acquisition using a scientific CMOS camera, high-precision XYZ translational stages, and programable light sources. The hardware is controlled using an in-house image acquisition software (vivoImager), is optimized for brightfield, fluorescence, and timelapse imaging of *C. elegans* immobilized within the vivoChip-24x device. This microfluidic device is operated using a dedicated controller (vivoCube+). **(B)** Each vivoChip-24x imaging experiment starts with preparing a config file, followed by acquiring data using vivoImager with vivoScreen hardware. Data is stored locally using 500+ TB network attached storage (NAS) and on cloud. A centralized, searchable database connects with all software modules and archives config and analysis files. Data is subsequently processed automatically to extract body parameters using a machine-learning (ML) model (vivoBodySeg [1]) and semi-automatically using a graphic user interface (vivoAnalyzer) for embryo phenotype analysis. The resulting data is then used for plots and statistical analyses.

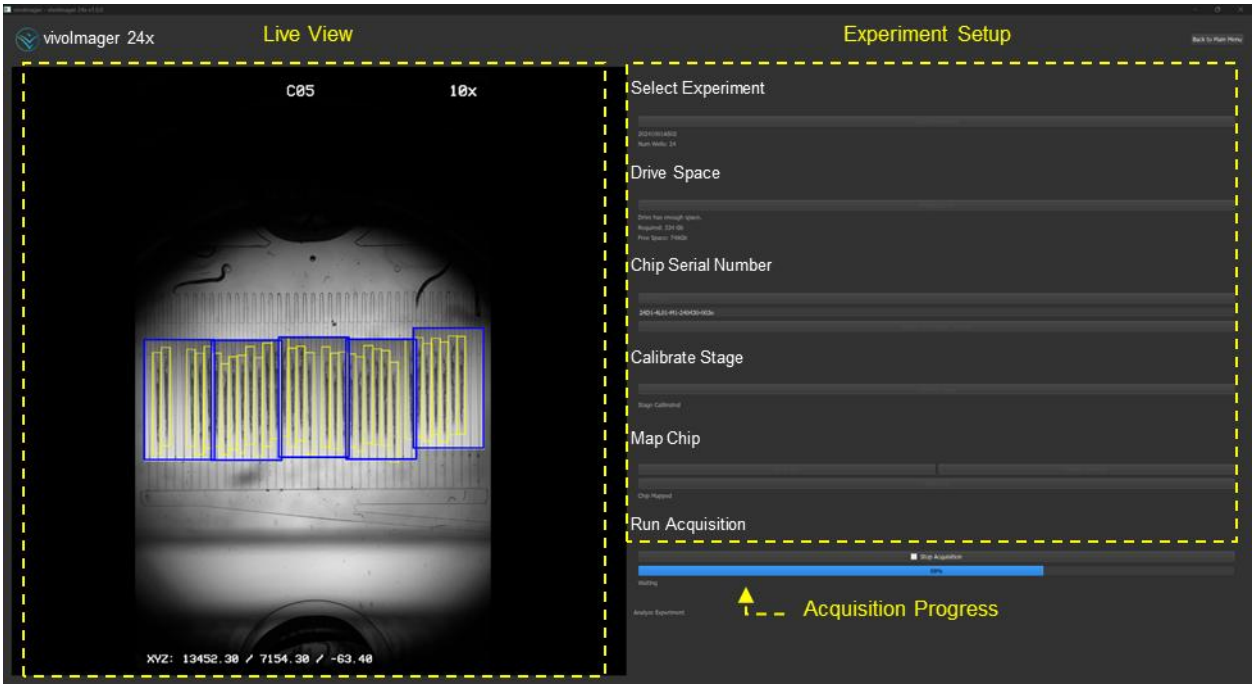

Supplementary Figure 2. Screenshot of the vivoImager software during automated imaging of a vivoChip-24x device. The software interface is organized into three main panels: (1) Experiment Setup Options, (2) Live View, and (3) Acquisition Progress. The Experiment Setup section guides the user through step-by-step process, starting with selection of a specific experiment config file and entry of the chip serial number. The program verifies that sufficient local storage is available before proceeding with the fully automated process for stage calibration, chip mapping, and data acquisition. The Live View panel displays 2× image of the well currently being imaged. Yellow boxes indicate individual bounding boxes identified by the YOLO-based detection model using 2× image. Based on these bounding boxes, the software predicts optimum positions for 5 field of views (FOVs, blue boxes) to capture all 40 channels. The Acquisition Progress panel displays real-time status updates as the software captures brightfield, fluorescence, or timelapse images from all 24 wells with 5 FOVs/well using the vivoChip-24x device.

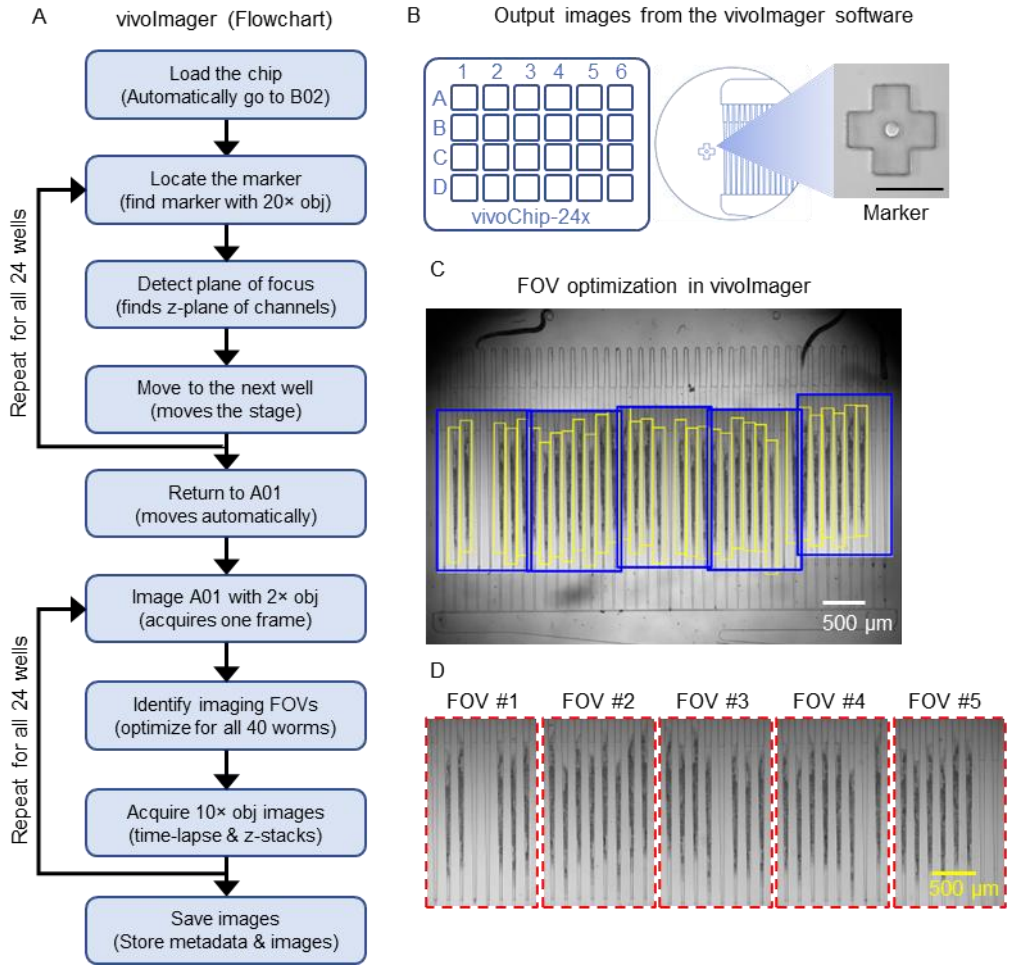

Supplementary Figure 3. vivoChip-24x automated imaging workflow. (A) Flowchart illustrating the automated imaging workflow. **(B)** Fiduciary cross markers positioned adjacent to each device are used to find the best focal plane prior to image acquisition. **(C)** Bounding boxes (yellow) corresponding to individual worms trapped within the microfluidic channels are identified using a worm-detection ML model applied to 2× objective (2× obj) images. Based on the detected worm positions, the software computes 5 FOVs that maximize centering of each group of 8 adjacent worms in xy within the imaging bounds of a 10× objective. The calculated FOV positions are overlaid as blue boxes on the 2× image. **(D)** The 5 FOVs capture all 40 channels at the optimal xy locations, enabling whole-body imaging for the majority of the *C. elegans* within the device.

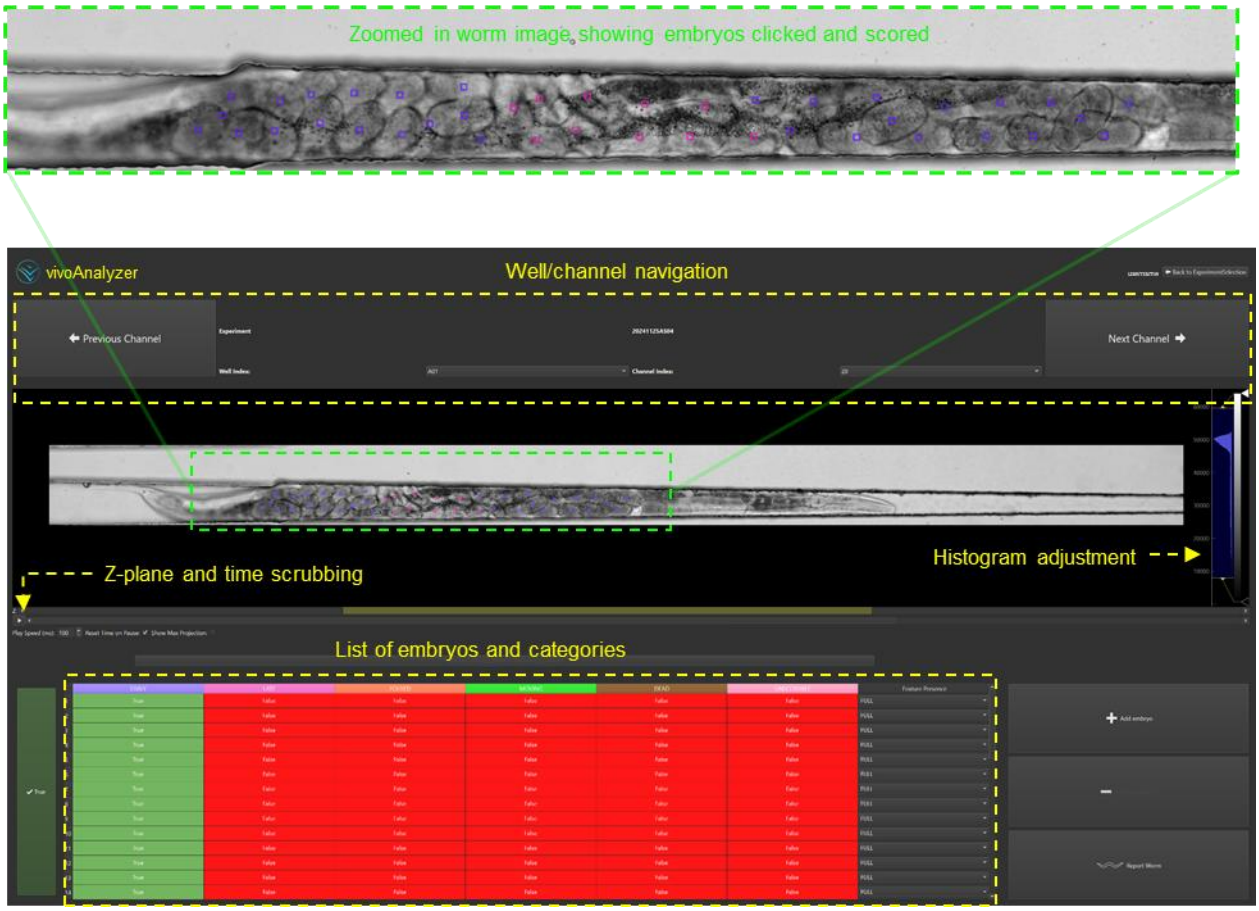

Supplementary Figure 4. Screenshot of the vivoAnalyzer software for embryo phenotyping. The vivoAnalyzer software is used to load individual imaging channels with worms for manual embryo scoring. Users can adjust the image histogram, scroll through the full z-stack, and zoom into specific regions in the image to facilitate accurate scoring and classification. When an embryo is identified, the user scores the embryo by clicking on the center of the embryo and assigns it to one of the 2 classifications: early-stage embryo or late-stage embryo. After scoring and classifying all embryos within a channel, the user proceeds to the next channel. All user inputs, including click coordinates (vertices), assigned classes (early, late, or none), and user metadata are stored in the centralized database. The vivoAnalyzer operates in two modes; (1) Normal Assignment Mode, in which the experiment name, well name, and channel numbers are visible to the user and (2) Blinded Assignment Mode, in which no identifying information about the channel image is displayed.

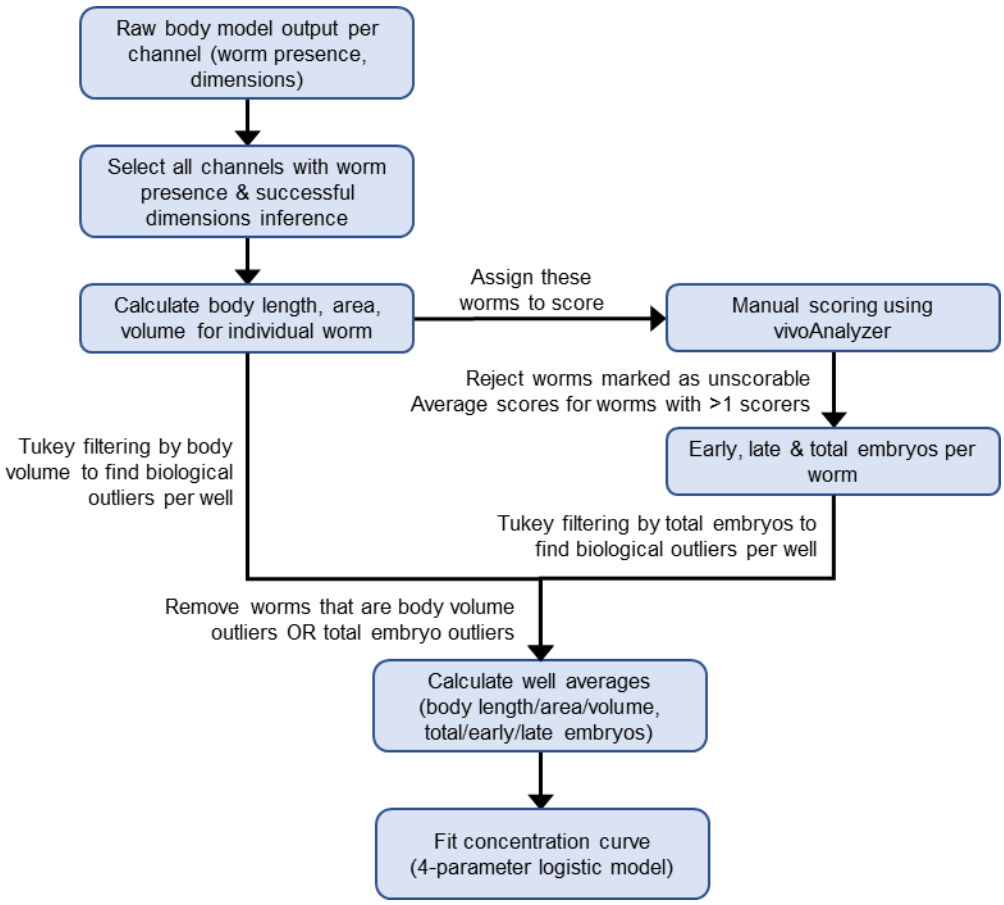

Supplementary Figure 5. Workflow of statistical analysis for body and embryo phenotypes. Raw outputs from body segmentation model, including the worm presence (full, partial, or none) and the predicted segmentation masks (vertices of the polygon, generated only for channels classified as "full") are stored in SQLite (SQLT) files in our NAS data storage system. The developmental parameters are subsequently extracted from the segmentation masks, as described in the Methods section. The channels with worms are scored manually to detect all *in utero* embryos and classified as early- or late-stage embryos. The manual scores are stored in the database. For each well, we identify the outliers for body volume and total embryos using Tukey filtering. The remaining channels are used to estimate well averages for 3 developmental (length, area, and volume) and 3 reproductive (total, early, and late embryos) parameters. The well averages are used to create concentration curves and fit 4-parameter logistic model to estimate effective concentrations.

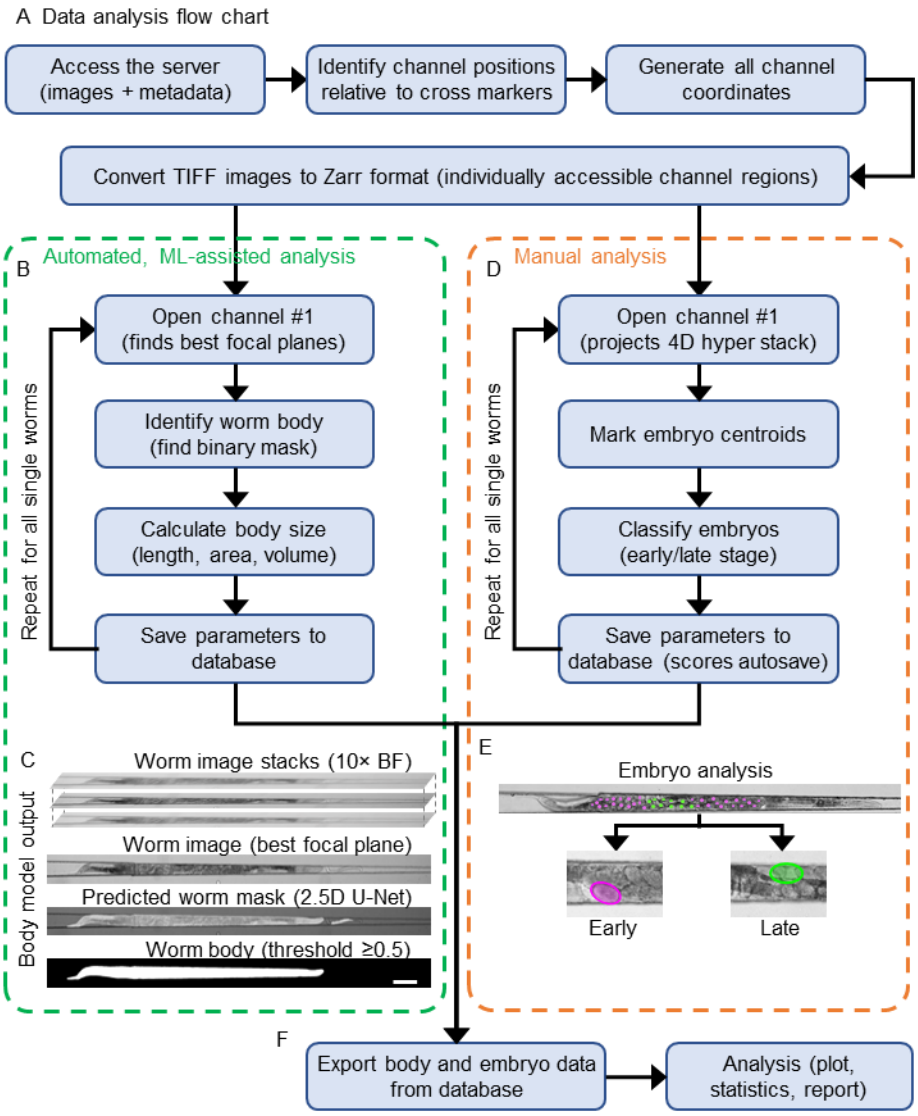

Supplementary Figure 6. An automated image acquisition and analysis pipeline to rapidly screen *C. elegans* models for DART studies. (A) Flowchart showing the image processing pipeline, beginning with accessing raw imaging data, identifying channel positions relative to fiduciary cross markers, and registering boundary coordinates for individual channels. The associated metadata are stored on the server. Raw TIFF stacks are converted to the Zarr format, which allows data-efficient access to image subsets corresponding to an individual channel withing the full FOV (8 channels per FOV). This format allows parallel read and write operations across multiple threads or processes, facilitating distributed computing frameworks necessary for high-speed analysis. **(B)** Overview of the automated, ML-assisted body segmentation process. The model selects the best 5 focal planes, predicts a body mask, generates a binary segmentation of the worm body outline, and computes body parameters including body length, area, and volume of the worm. **(C)** Representative images of a worm within a single channel showing the steps of automated ML-assisted body segmentation (finding the best focus plane from the z-stack, predicting body pixels using the trained model, and generating a binary mask by thresholding pixels with a probability >0.5 of belonging to the worm body). Scale bar is 100 µm. **(D)** Overview of the manual

embryo phenotyping workflow, in which trained human scorers label and categorize all embryos within the germline of each worm. **(E)** Representative images of an individual worm showing the embryo scoring (marking the centroid) and classification (early- or late-stage embryo) by human users. **(F)** Scoring and classification data from each experiment is stored in a database and can be exported for plotting and statistical analysis.

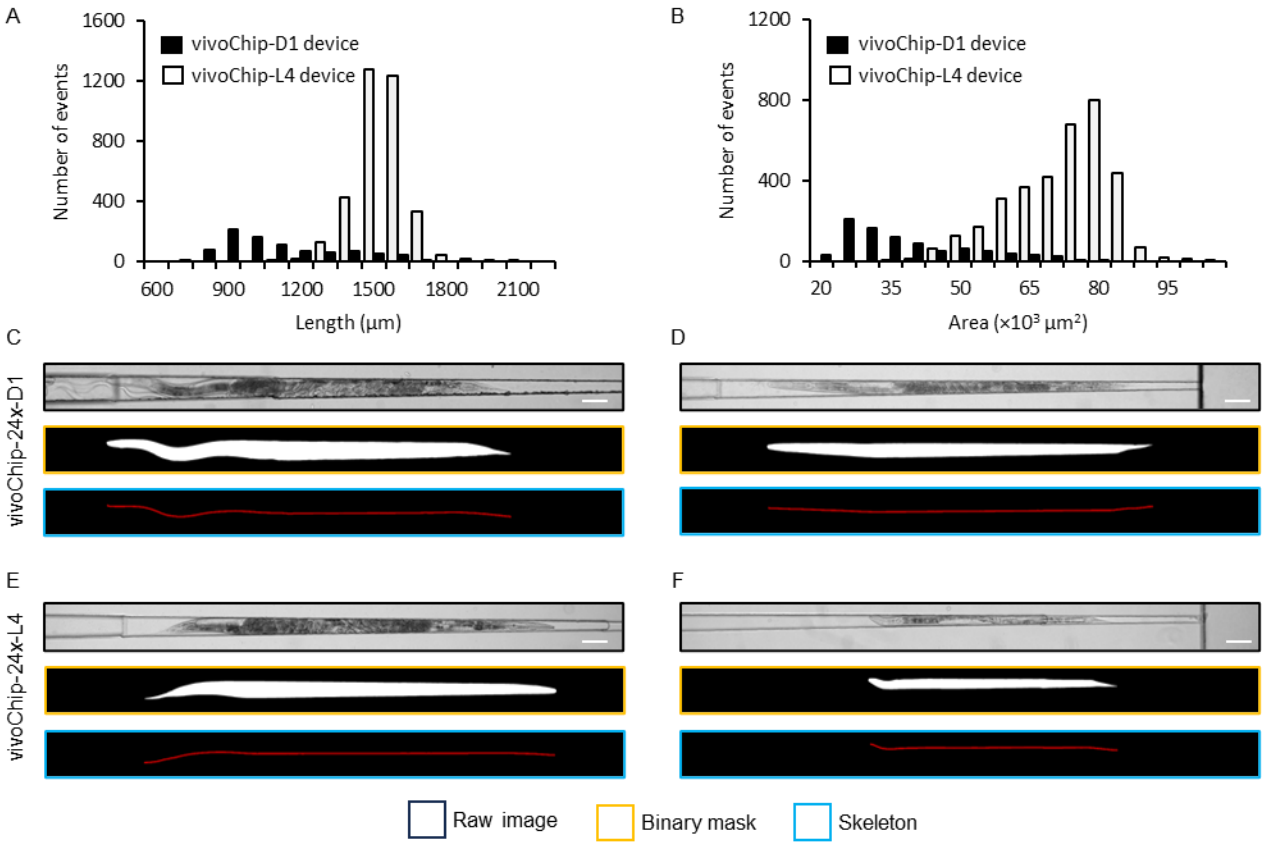

Supplementary Figure 7. Dataset for U-Net-based body segmentation model. The training dataset consists of *n* = 4,360 channels, manually classified as full and segmented for the worm bodies. **(A-B)** Histogram plot of body length (A) and area (B) quantified from the manually segmented body masks. **(C-F)** Example images of worms immobilized in the vivoChip-24x-D1 (C-D) and vivoChip-24x-L4 (E-F) devices.

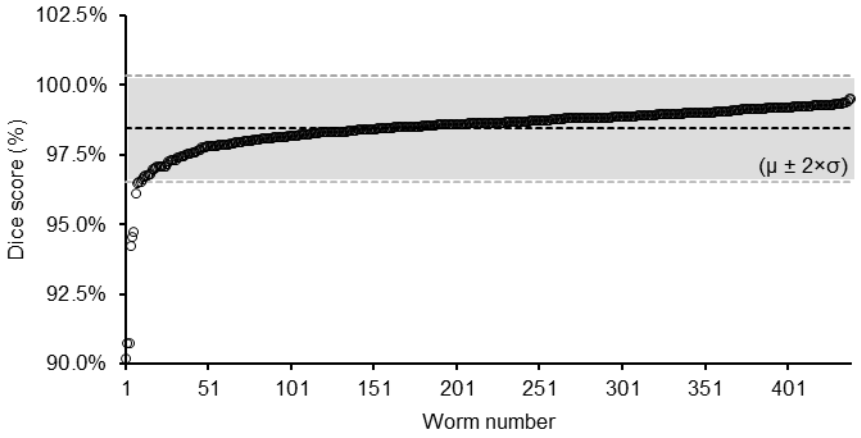

Supplementary Figure 8: Dice score for the predicted worm segmentation. The Dice score for all 439 test channels with full worms are arranged with worm numbers representing low to high Dice scores. The grey area represents the mean ± 2×standard deviation (μ ± 2σ) values for the Dice score. Only 8 channels were below 96.5% (μ - 2σ) dice score.

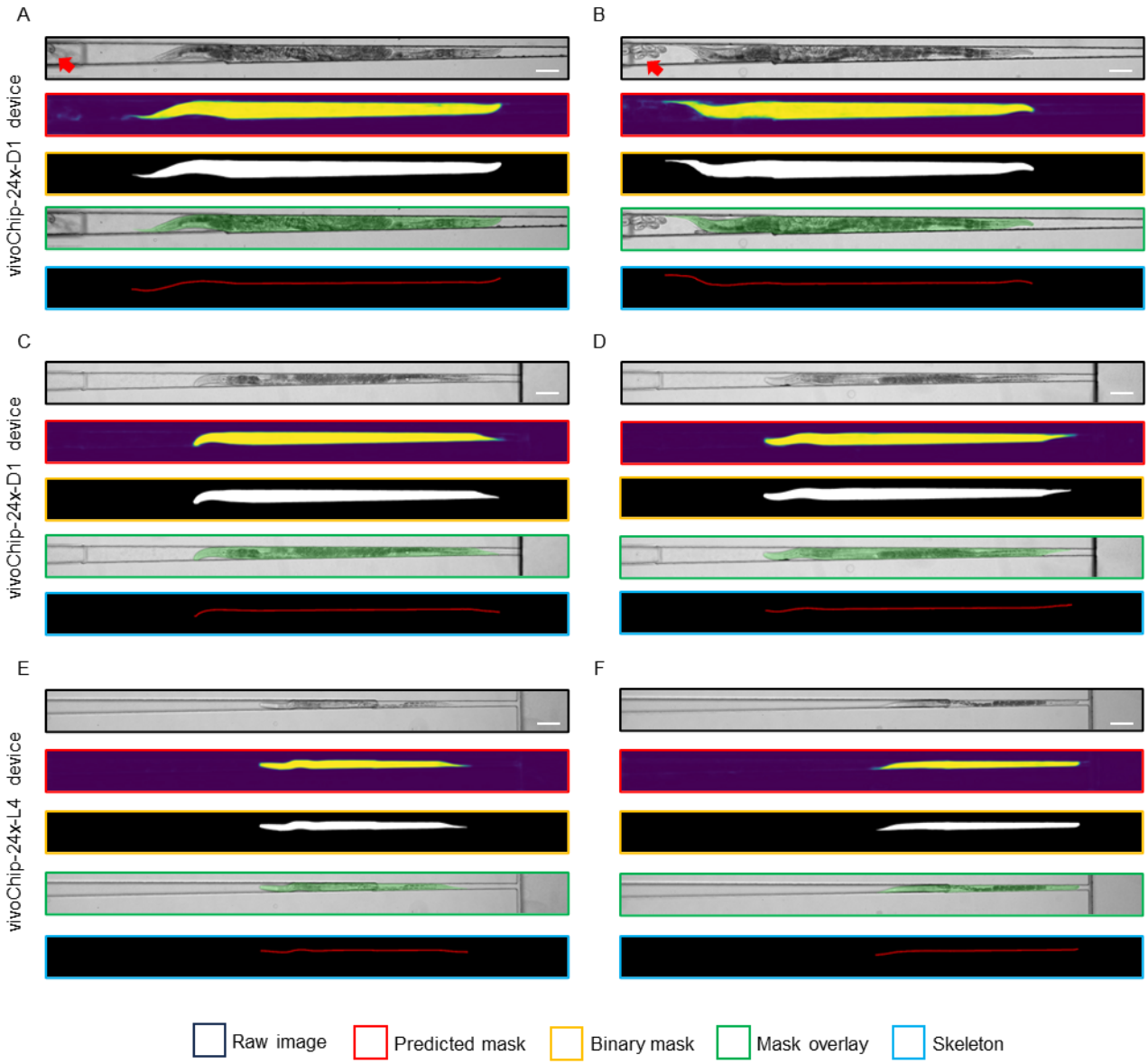

Supplementary Figure 9: Example of *C. elegans* body segmentation. (A-D) Example worm imaged using vivoChip-24-D1 device. **(E-F)** Example worm imaged using vivoChip-24-L4 device. The image shows the raw image, predicted mask, binary mask, overlaid mask, and skeleton. The skeleton is used for body length estimate (red line), region within the binary mask is used to estimate body area, and channel height is used for volume calculation. The red arrow indicates an unhatched egg inside the channel, which is ignored since it is outside the large worm body mask. The scale bar = 200 µm.

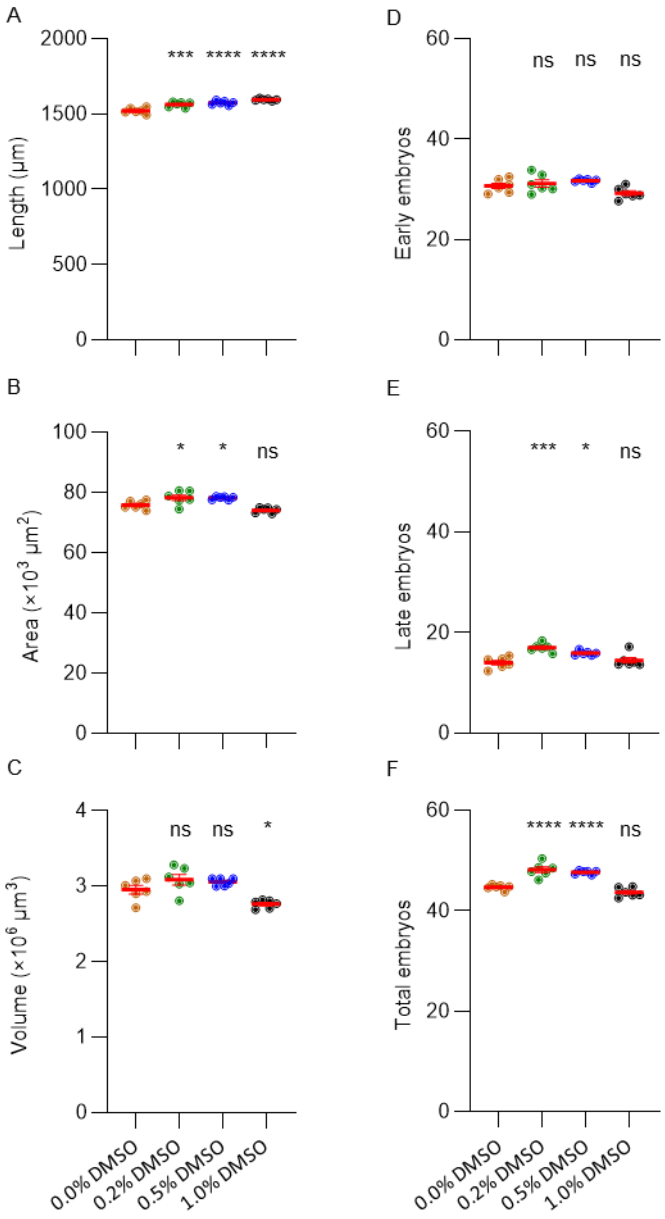

Supplementary Figure 10. Well averages for all 6 DART parameters from one of the biological replicates. Scatter plots showing well averages from all 24 wells for the biological replicates, presented in Figure 3. **(A-C)** Scatter plot for body length (A), area (B), and volume (C). **(D-F)** Scatter plot for early embryos (D), late embryos (E), and total embryos (F). The red lines indicate mean ± SEM. One-way ANNOVA was used to compare the mean values (n = 6 technical replicates) for 0.2%, 0.5%, and 1.0% conditions with respect to 0.0% DMSO wells. The p-values are indicated as ns (p-value ≥ 0.05), * (p-value ≥ 0.05), ** (p-value ≤ 0.01), *** (p-value ≤ 0.001), and **** (p-value ≤ 0.0001).

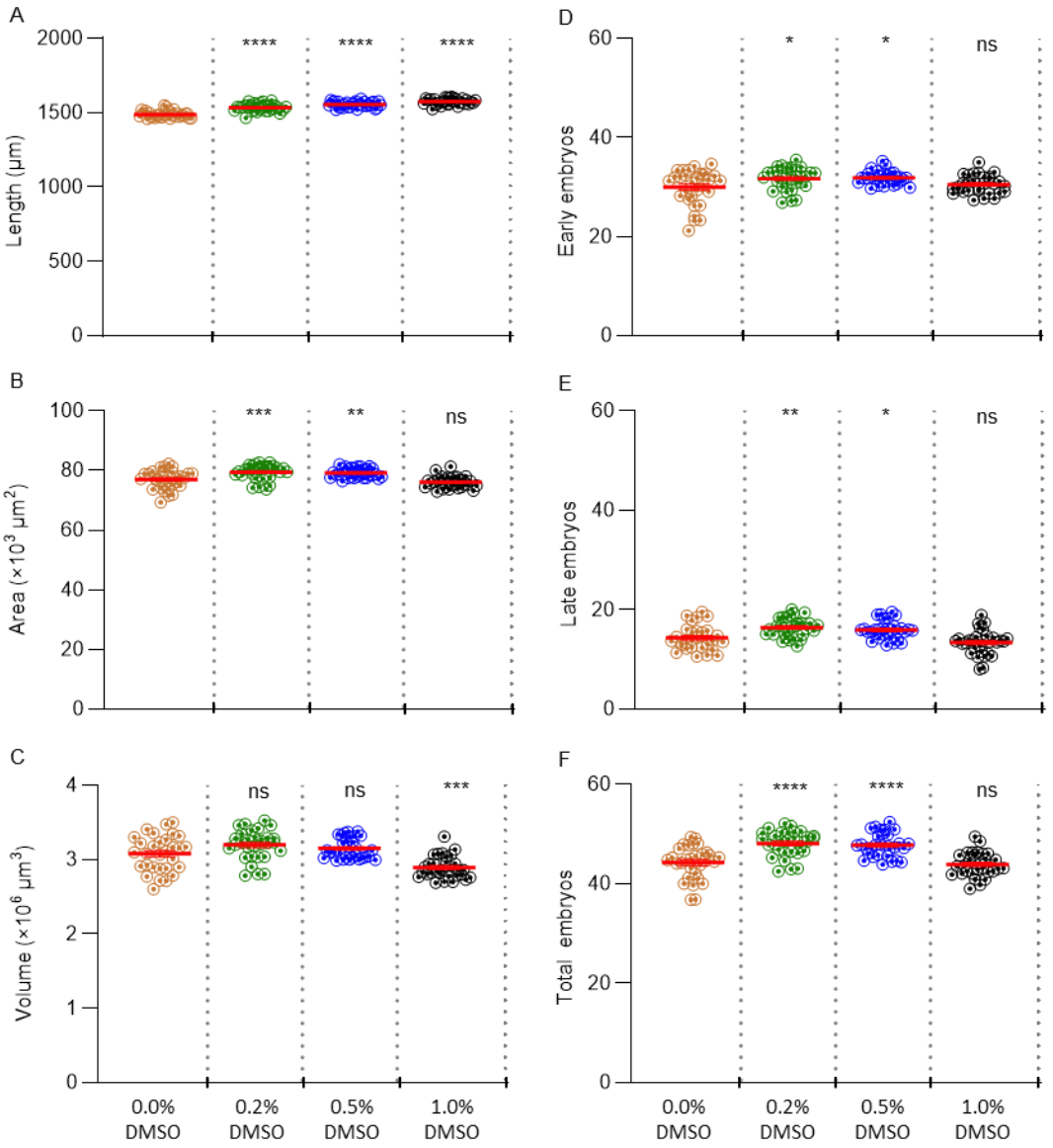

Supplementary Figure 11. Variation in DART parameters across worms treated with four solvent conditions and five biological replicates. Scatter plots showing all 30 well averages (5 biological replicates × 6 technical replicates) for 6 DART-related parameters under four DMSO conditions (0% = Brown, 0.2% = Green, 0.5% = Blue, and 1% = Black). **(A-C)** Scatter plot for body length (A), area (B), and volume (C). **(D_F)** Scatter plot for early embryos (D), late embryos (E), and total embryos (F). The red lines indicate mean ± SEM. One-way ANNOVA was used to compare the mean values (*n* = 30 wells each) for 0.2%, 0.5%, and 1.0% conditions with respect to 0.0% DMSO wells. The *p*-values are indicated as ns (*p*-value ≥ 0.05), * (*p*-value ≥ 0.05), ** (*p*-value ≤ 0.01), *** (*p*-value ≤ 0.001), and **** (*p*-value ≤ 0.0001).

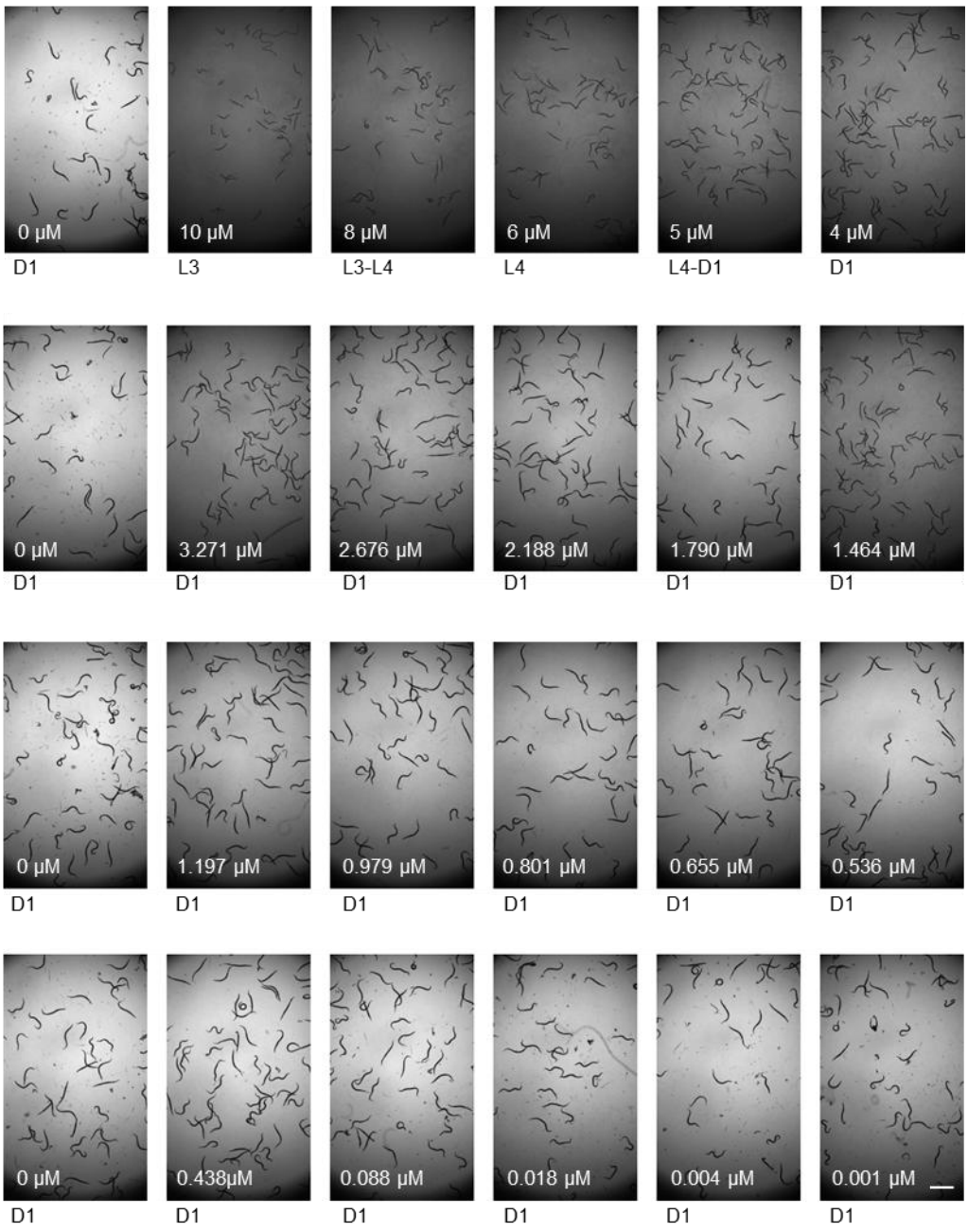

Supplementary Figure 12: Range-finding assay with methylmercury. Worms were treated to increasing concentrations of methylmercury as indicated in the image. The worm developmental stages were manually assessed and the average stage for each condition is shown below the corresponding image. Wells containing worms below the L4 stage were not loaded into the vivoChip-24x device (adult device or L4 device) for high-resolution imaging. Adult worms from 0 up to 4 µM conditions were loaded in the vivoChip-24x (adult device), whereas worms from higher than 4 µM condition were loaded into the vivoChip-24x (L4 device). The scale bar is 200 µm.

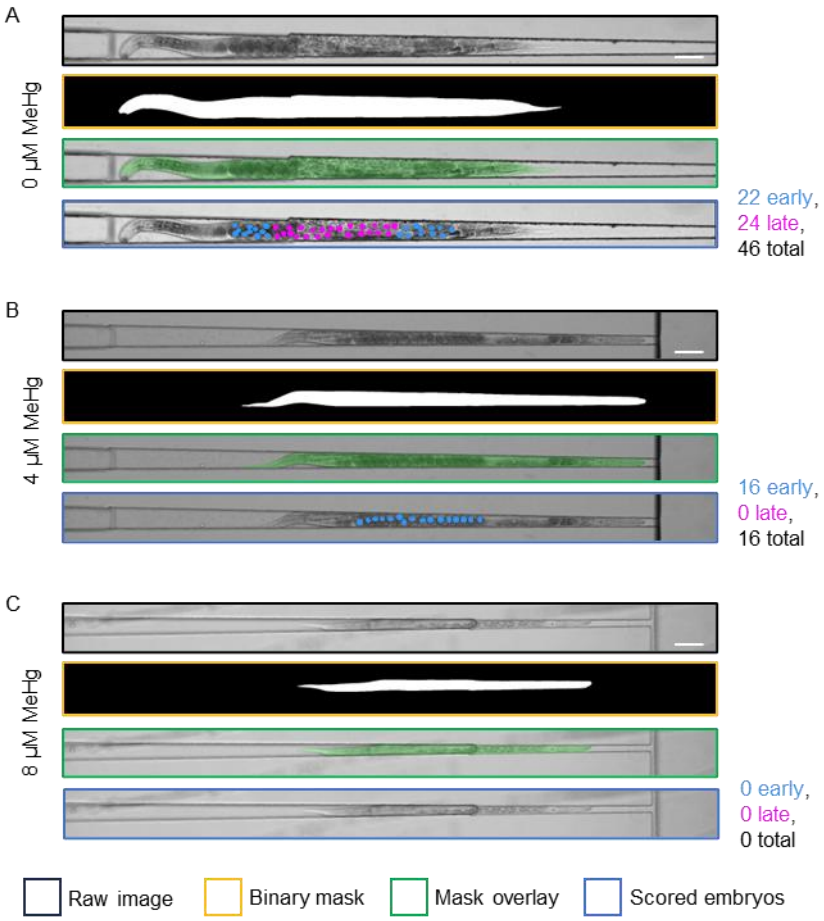

Supplementary Figure 13: Representative images of methylmercury-treated worms. (A-C) Statistically representative example worms selected based on body volume for 0 µM, 4 µM and 8 µM methylmercury (MeHg) treatment conditions. For each channel, the raw image is shown along with the corresponding binary mask predicted by the ML model inference. The third image shows the green-colored overlay of the mask on the worm body. The manually annotated embryo locations and classifications are also shown (blue dots = early-stage embryos and magenta dots = late-stage embryos). Adult worms from the 0 µM and 4 µM conditions were loaded in the vivoChip-24x (adult device), whereas L4-stage worms from the 8 µM condition were loaded into the vivoChip-24x (L4 device). Scale bar is 100 µM.

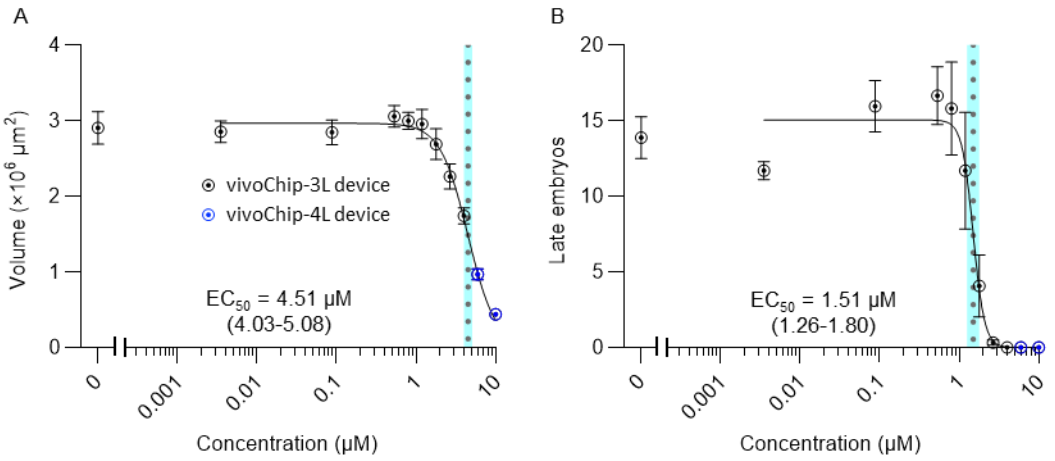

Supplementary Figure 14: Concentration-response curve for methylmercury with 10 concentrations. **(A-B)** The effects of methylmercury on body volume (A) and late-stage embryos (B). We skipped every other data presented in Figure 7 and were used to create a 10-point concentration-response curve for methylmercury. Data from 3 biological replicates were performed using either D1 (black circle) or L4 (blue circles) chips. The combined well average values from both datasets were fitted with a 4-parameter logistic curve (solid black lines). The EC_{50} estimates are indicated with dotted lines with corresponding 95% confidence interval bands shaded in light-blue color.

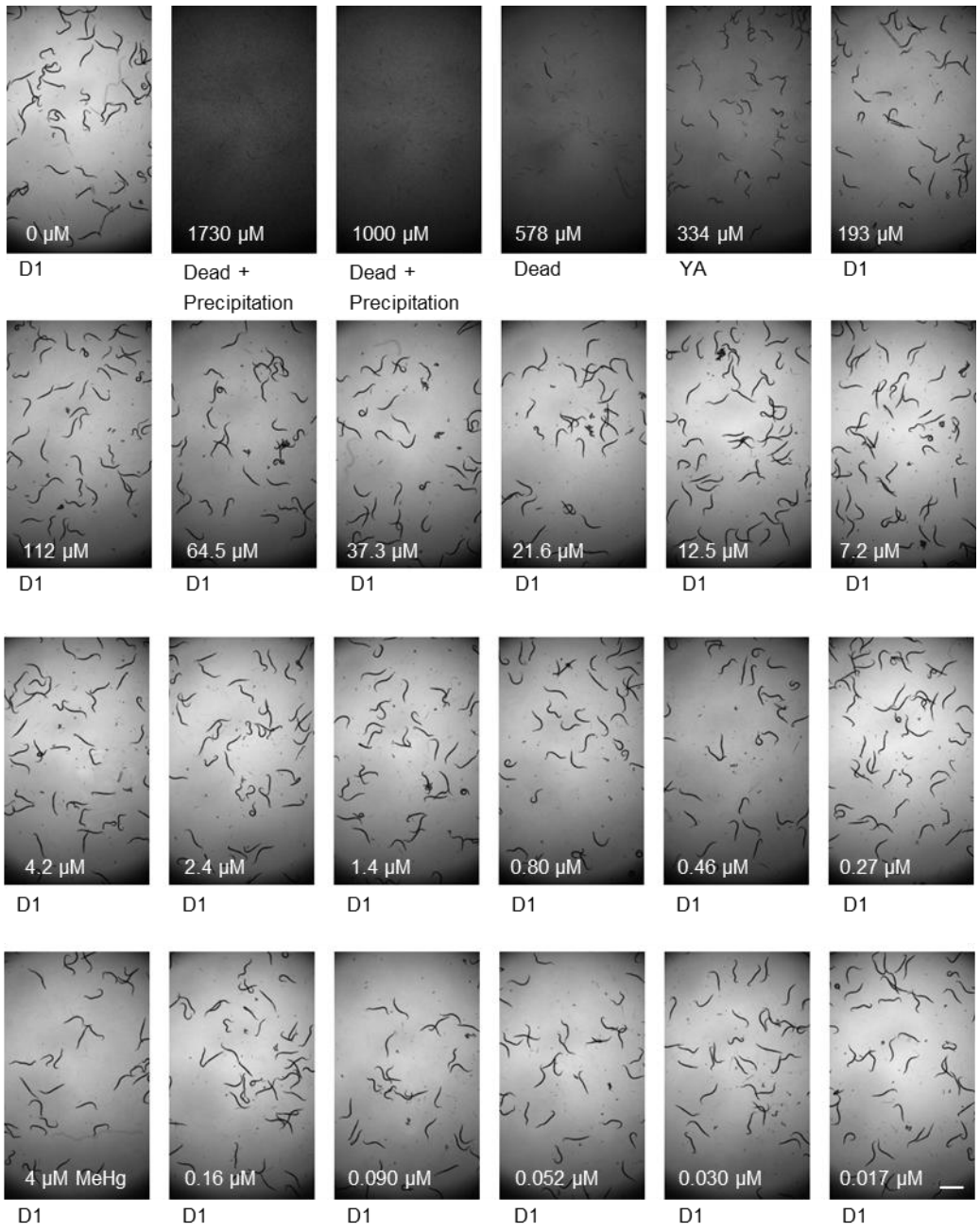

Supplementary Figure 15: Range-finding assay with propiconazole. Worms were treated to increasing concentrations of propiconazole as indicated in the image. The worm developmental stages were manually assessed, and the average stage for each condition is labelled below the corresponding image. Dead worms and any observed precipitation of propiconazole in the culture medium are also indicated. Wells containing worms below the L4 stage were not loaded into the vivoChip-24x device (adult device or L4 device) for high-resolution imaging. Adult worms from 0 up to 193 µM conditions were loaded in the vivoChip-24x (adult device), whereas worms from 334 µM was loaded into the vivoChip-24x (L4 device). The scale bar is 200 µm.

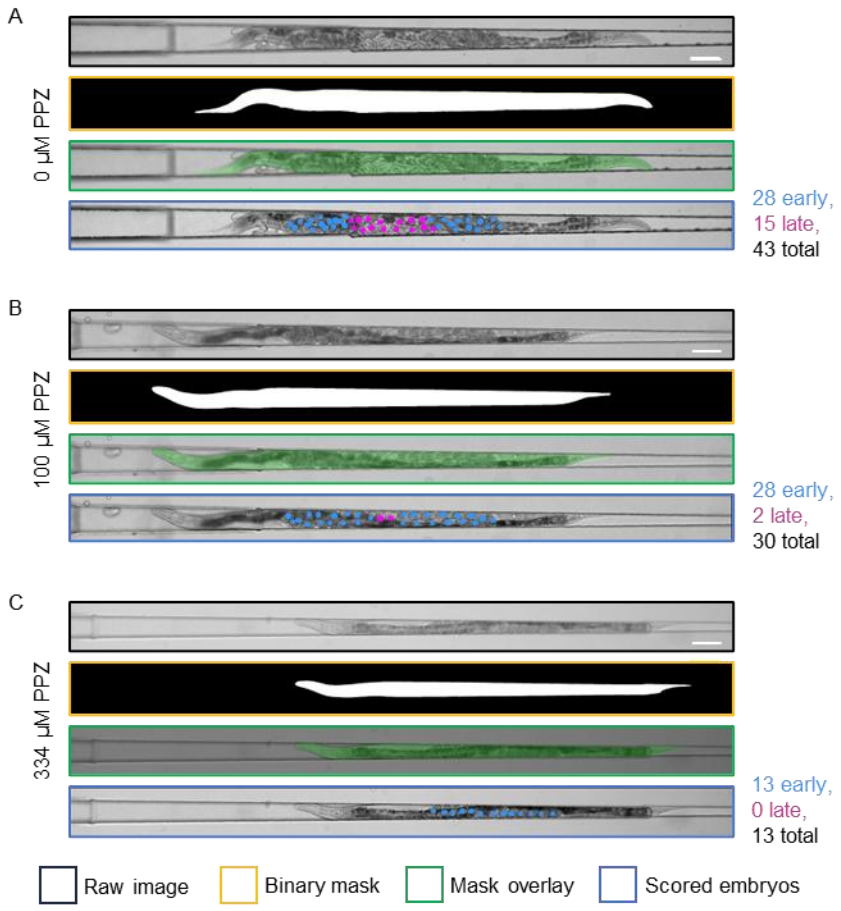

Supplementary Figure 16: Representative images of propiconazole-treated worms. (A-C) Statistically representative example worms selected based on body volume for 0 µM, 100 µM and 334 µM propiconazole (PPZ) treatment conditions. For each channel, the raw images are shown along with the binary mask predicted by the ML model inference. The third image shows the green-colored overlay of the mask on the worm body. Manually annotated embryo locations and classifications are also shown (blue dots = early-stage embryos and magenta dots = late-stage embryos). Adult worms from the 0 µM and 100 µM conditions were loaded into the vivoChip-24x (4L device), whereas worms from the 334 µM condition were loaded into the vivoChip-24x (D1 device), as approximately 34% of this worm population was below the minimum size that could be reliably trapped in the vivoChip-24x (L4 device). Scale bar is 100 µM.

Supplementary Table 1: Predefined assay acceptance criteria for DART experiments.

Parameter	Acceptance Criterion	Notes
Number of P_0 worms per experiment	4 L4 worms per plate, 2 plates per experiment	Transfer manually using standard picking technique
Removing of P_0 adults	All 4 P_0 adults removed from each plate at 48 hours	Terminate experiment if any P0 adult is missing
Bleaching efficiency	≥ 5,000 embryos obtained ≥ 50% hatching efficiency	Use synchronized L1s within 24 hours of bleaching
Number of L1s per well	80-100 L1s per well	Count prior to plating
Food concentration in the *C. elegans* liquid culture	OD_{600} = 3.0 ± 0.1	Measure the HB101 stock resuspended in S media using spectrophotometer
Incubator temperature	20 ± 0.1 °C	Monitor hourly via temperature sensor
Incubator humidity	40 – 60%	Monitor hourly via humidity sensor
C. elegans development in the solvent control	Worms in the vehicle control reach D1 adulthood	Manually verify worm number and developmental stages using a 2× objective
vivoChip imaging window	Capture vivoChip images 72 ± 1 hours after plating	Maintain consistent imaging time to reduce variability in DART parameters
Reference chemicals	Purchased from qualified vendor with documented batch number and Certificate of Analysis (CoA)	Follow vendor-specified storage and safety instructions
Master stock preparation	Prepare high concentration master stocks and store them at -80 °C for long-term storage and use	Prepare single use aliquots using DMSO or appropriate solvents
Working stock preparation	Prepare 200× fold dilutions for treatment	Store and use working stocks up to 3 days at 4 °C

Supplementary Table 2. Effective concentration values for DART-related parameters for methylmercury-treated worms. The EC_{10}, EC_{25}, and EC_{50} and 95% confidence interval (95% CI) are calculated for all six parameters**.**

Parameters	**EC_{50} (95% CI)**	**EC_{25} (95% CI)**	**EC_{10} (95% CI)**
Length	8.22 µM (7.83-8.69)	4.90 µM (4.65-5.15)	2.92 µM (2.65-3.18)
Area	5.33 µM (4.98-5.72)	3.21 µM (2.91-3.52)	1.93 µM (1.63-2.24)
Volume	4.61 µM (4.28-4.99)	2.93 µM (2.62-3.26)	1.86 µM (1.56-2.20)
Early embryos	3.90 µM (3.66-4.16)	3.26 µM (2.98-3.54)	2.72 µM (2.38-3.08)
Late embryos	1.49 µM (1.33-1.67)	1.25 µM (1.07-1.42)	1.04 µM (0.82-1.26)
Total embryos	3.14 µM (2.90-3.38)	2.32 µM (2.07-2.58)	1.72 µM (1.44-2.01)

Supplementary Table 3. Effective concentration values for DART-related parameters for methylmercury-treated worms with 10 concentrations. The EC_{10}, EC_{25}, and EC_{50} and 95% confidence interval (95% CI) are calculated for all six parameters**.**

Parameters	**EC_{50} (95% CI)**	**EC_{25} (95% CI)**	**EC_{10} (95% CI)**
Length	7.99 µM (7.4-8.75)	4.8 µM (4.43-5.18)	2.88 µM (2.49-3.28)
Area	5.2 µM (4.71-5.79)	3.2 µM (2.75-3.66)	1.97 µM (1.52-2.45)
Volume	4.51 µM (4.03-5.08)	2.91 µM (2.43-3.41)	1.88 µM (1.4-2.41)
Early embryos	3.87 µM (3.51-4.24)	28 µM (2.76-3.71[a])	2.7 µM (2.06-3.35[a])
Late embryos	1.51 µM (1.26-1.80)	1.26 µM (0.93-1.58[a])	1.05 µM (0.65-1.45[a])
Total embryos	3.08 µM (2.72-3.47)	2.27 µM (1.87-2.68)	1.67 µM (1.23-2.13)
[a]The 95% CI is calculated using symmetric asymptote.			

Supplementary Table 4. Strictly Standardized Mean Difference values for different concentrations of methylmercury. Strictly Standardized Mean Difference (SSMD) values were calculated by comparing the mean control wells for each treatment across 3 independent experiments for every methylmercury (MeHg) concentration. Green shading indicates excellent assay quality for a strong effect (SSMD ≥ 2).

MeHg (µM)	Length	Area	Volume	Early	Late	Total
10						
8	10.70	7.29	5.52	11.38	5.84	9.77
6	9.16	6.29	4.87	9.00	5.84	8.82
5	10.92	5.41	4.08	7.12	5.84	7.65
4	5.18	3.24	2.77	2.96	5.84	4.73
3.2714	3.58	2.40	2.12	1.05	5.74	3.04
2.6755	0.53	1.41	1.35	0.10	5.66	1.61
2.1882	-0.29	0.99	1.00	-0.32	3.53	1.00
1.7896	-0.91	0.34	0.41	-2.05	2.30	0.30
1.4636	-1.18	0.09	0.08	-2.37	1.03	-0.43
1.197	-2.05	-0.09	-0.10	-1.04	0.31	-0.30
0.979	-2.53	-0.24	-0.18	-0.64	-0.29	-0.49
0.8007	-3.42	-0.33	-0.22	-0.31	-0.33	-0.45
0.6548	-1.03	-0.38	-0.28	-0.67	-0.17	-0.57
0.5356	-1.89	-0.33	-0.34	-0.40	-0.68	-0.66
0.438	-1.23	-0.07	-0.02	-0.02	-0.62	-0.37
0.0876	-0.88	0.06	0.12	-1.09	-0.55	-0.89
0.0175	-0.57	0.11	0.19	-0.31	0.14	-0.11
0.0035	-0.79	0.00	0.12	-0.72	0.84	-0.08
0.0007	-0.86	0.07	0.19	-0.46	0.05	-0.21

Supplementary Table 5. Effective concentration values for DART-related parameters for propiconazole-treated worms. The EC_{10}, EC_{25}, and EC_{50} and 95% confidence interval (95% CI) are calculated for all six parameters**.**

Parameters	**EC_{50} (95% CI)**	**EC_{25} (95% CI)**	**EC_{10} (95% CI)**
Length	504 µM (392-685)	345 µM (320-388)	237 µM (192-294)
Area	384 µM (359-418)	223 µM (207-240)	130 µM (111-149)
Volume	336 µM (311-369)	188 µM (169-207)	105 µM (86-125)
Early embryos	252 µM (230-276)	154 µM (132-175)	94 µM (72-117)
Late embryos	78 µM (35-154)	33 µM (6-93)	14 µM (1-65)
Total embryos	204 µM (177-237)	109 µM (83-137)	58 µM (36-85)

References:

1. DuPlissis, A., et al., *Machine learning-based analysis of microfluidic device immobilized C. elegans for automated developmental toxicity testing*. Sci Rep, 2025. **15**(1): p. 15.